

2 Indications for aggravation in summer heat conditions over the 3 Mediterranean Basin

4 Baruch Ziv,¹ Hadas Saaroni,² Anat Baharad,³ Daniel Yekutieli,⁴ and Pinhas Alpert³

5 Received 23 February 2005; revised 11 April 2005; accepted 27 April 2005; published XX Month 2005.

7 [1] The summer temperature variations over the
8 Mediterranean Basin were studied through the 850 hPa
9 level for the months June–August along the period 1948–
10 2003, based on the NCEP-NCAR CDAS-1 archive. The most
11 prominent feature found is warming, larger than the global
12 value, over the majority of the study region with a maximum
13 of 0.04 Ky^{-1} over Sicily. At the same time, cooling was noted
14 over Algeria and the Balkans. The trend for the 10% upper
15 quantile of the days over the warming region was found
16 larger than the seasonal, reaching 0.053 Ky^{-1} , implying that
17 heat waves lead the general long-term trend. The shape of the
18 long-term curve was found to fit the global one over the
19 warming region. No synoptic-dynamic factor was found to
20 account for the intensity and spatial distribution of the
21 warming trend. This, together with the fit of the trend with the
22 global one, suggests that the Mediterranean Basin manifests
23 the increase in the greenhouse effect in the summer season.

24 **Citation:** Ziv, B., H. Saaroni, A. Baharad, D. Yekutieli, and
25 P. Alpert (2005), Indications for aggravation in summer heat
26 conditions over the Mediterranean Basin, *Geophys. Res. Lett.*, 32,
27 LXXXXX, doi:10.1029/2005GL022796.

29 1. Introduction

30 [2] A global warming trend has been noted for the last
31 century, in particular along the last 3 decades, though varying
32 considerably in space and season [*Intergovernmental Panel
33 on Climate Change (IPCC)*, 2001]. The warming trend of
34 the summer surface air temperature over the Mediterranean
35 Basin (MB) and southern Europe for the period 1950–1999
36 was 0.008 Ky^{-1} [*Xoplaki et al.*, 2003], and reached the value
37 of 0.01 Ky^{-1} for 1976–2000 [*IPCC*, 2001, Figure 2.10c],
38 one of the highest rates over the entire globe. The high
39 summer average daily maximum temperatures along the
40 Mediterranean dense populated coastal plains, reaching
41 30°C , combined with the high relative humidity [*Wallen,
42 1977*], implies that heat stress conditions prevail there.
43 Therefore, any further warming in this region has far reach-
44 ing environmental implications, so that the long-term trend
45 of the temperature regime in this sensitive region needs to be
46 investigated in detail.

¹Department of Natural Sciences, Open University of Israel, Tel-Aviv, Israel.

²Department of Geography and the Human Environment, Tel-Aviv University, Tel-Aviv, Israel.

³Department of Geophysics and Planetary Sciences, Tel-Aviv University, Tel-Aviv, Israel.

⁴Department of Statistics and Operations Research, Tel-Aviv University, Tel-Aviv, Israel.

[3] During the last two decades Western Europe suffered 47
48 from severe summer heat waves with extreme maximum
49 values on the summer of 2003 [*Le Comte*, 2004; *Luterbacher
50 et al.*, 2004; *Meehl and Tebaldi*, 2004]. The spatial distribu-
51 tion of the 925 hPa level temperature anomaly for June–
52 August 2003 over the MB (based on NCEP/NCAR data
53 base; Figure 1) shows a maximum of over 4.5° over the
54 western Mediterranean region. Similar results were obtained
55 for the surface and 850 hPa levels.

[4] The long-term trend in the temperature regime over 56
57 the MB, covering 25°N – 45°N , 0° – 40°E , is studied along
58 the period 1948–2003 for the months June, July and August
59 (JJA), using the 850 hPa level. Following *Saaroni et al.*
60 [2003], we chose the 850 hPa level as representing the
61 lower-levels, because it is not overly sensitive to near
62 surface effects, such as the urban effects (as shown by
63 *Kalnay and Cai* [2003]). The database is the NCEP-NCAR
64 CDAS-1 archive [*Kalnay et al.*, 1996; *Kistler et al.*, 2001].

[5] Section 2 presents the long-term trend of the seasonal 65
66 temperature and compares their temporal variations with the
67 yearly global trend. Section 3 examines the trend of
68 extremity, concentrating on the contribution of heat waves,
69 and the last section discusses and summarizes the results.

2. Long-Term Trend of the Seasonal Average Temperature

[6] The spatial distribution of the long-term linear trend of 72
73 the seasonal temperature was extracted by mapping the
74 slope of the best-fit straight line for each grid point along
75 the study period (Figure 2). A warming trend was found
76 over the majority of the MB. Two pronounced maxima can
77 be noted. The most pronounced one is at the western
78 Mediterranean (0.04 Ky^{-1} maximum) and the second over
79 northern Egypt (0.034 Ky^{-1} maximum). In addition, two
80 weak negative centers, reflecting a cooling trend, were
81 found over the Balkans (-0.008 Ky^{-1}) and over Algeria
82 (-0.015 Ky^{-1}). The cooling over the Balkans is consistent
83 with the significant cooling over Greece along 1951–1985
84 found by *Reddaway and Bigg* [1996]. A similar distribution
85 was found for each of the 3 individual months, among
86 which the most extreme values were obtained for July
87 (0.047 Ky^{-1} maximum). Figure 3 shows the spatial distri-
88 bution of the confidence-level of the linear trend. The area
89 that has the maximum confidence level, >0.95 , is rather
90 similar to that which experience the most intense warming
91 (Figure 2). In addition, high confidence level (>0.95) is
92 found in the middle of the cooling region over Algeria.

[7] In order to examine the course of the temperature 93
94 trend the curve that best fits the temperature time series
95 was derived for each grid point in the study area, using
96 the locally weighted scatter-plot smoother (LOWESS)

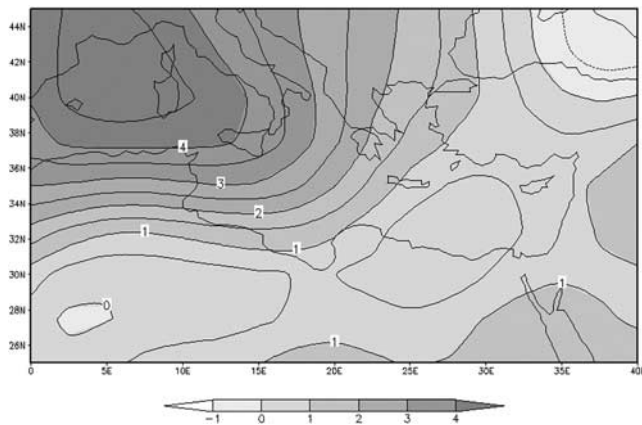


Figure 1. 925 hPa temperature anomaly for JJA, 2003, based on the NCEP-NCAR CDAS-1 archive [Kalnay et al., 1996; Kistler et al., 2001]. See color version of this figure in the HTML.

[Chambers et al., 1983; Cleveland, 1979], belonging to “S-plus” functions (S-PLUS[®] 6.2 for Windows, copyright 1988, 2003 Insightful Corp.). A window, depending on an f -parameter, i.e., the fraction of data smoothed around each point, is placed about each x value. Points that are inside the window are weighted so that those nearby points get the largest weights. In general, the larger the f , the smoother is the fit. Here we used $f = 0.8$. The same procedure was applied to the mean global annual temperature time series for 1950–2001 [IPCC, 2001].

[8] The global yearly curve (Figure 4a) shows a slow warming trend from 1950 to the early seventies, with a slope of $\sim 0.003 \text{ Ky}^{-1}$, when it turns and attains a slope of $\sim 0.016 \text{ Ky}^{-1}$ for the period beginning at 1974 and ending at 2001. Figure 4b shows the spatial distribution of the seasonal long-term trend curves for the grid points over the study region. The region in which the curve shape is similar to the global one overlaps, more or less, that where the maximum warming rate was found (Figure 2). This region covers the majority of the MB and to its south, especially along its eastern part, where north-westerly winds

prevail [e.g., Ziv et al., 2004]. The region in which the long-term curve shows the inverse shape of the global one (sloping up along the first part of the study period, then turning down) almost coincides with the cooling region found over Algeria.

[9] The degree of similarity between the global and the MB long-term trends was further examined by correlation maps between the seasonal time-series at each grid point in the study region and the global yearly ones (not shown). The correlation yielded positive values over the majority of the study region with two maxima, $>+0.64$ over Egypt and >0.5 over the western Mediterranean, the regions where the highest warming trends were found. Negative values were found over Algeria, where negative trend was observed. When the time-series were smoothed, the distribution remained the same and the amplitude increased. When each individual temperature was replaced by the 9-year moving average the positive correlation over the MB attained $+0.9$ (over its western part) and -0.78 over Algeria.

[10] The above findings indicate that in the summer season the MB has an affinity to the global temperature course in two aspects: one is the sign of the long-term linear trend (but with a higher rate) and second is the shape of the trend curve.

3. Extremity and Contribution of Heat Waves

[11] The environmental aspects of the warming trend are not fully captured by the average seasonal temperatures alone, but also by analyzing the occurrences of hot events (heat waves). These are represented here by the 10% upper quantile of the days. The spatial distribution of the long-term trend for these days (Figure 5) is similar to that of the seasonal average (Figure 2), except for larger amplitude, e.g., a maximum of 0.053 Ky^{-1} , as compared to 0.04 Ky^{-1} for the seasonal average (western Mediterranean), and -0.017 Ky^{-1} against -0.009 Ky^{-1} (Algeria). As was found for the average monthly temperature, the trend of the 10% upper quantile was the largest in July, being 0.069 Ky^{-1} over Sicily. This emphasizes that the increase in the frequency of heat waves play a central role in the warming

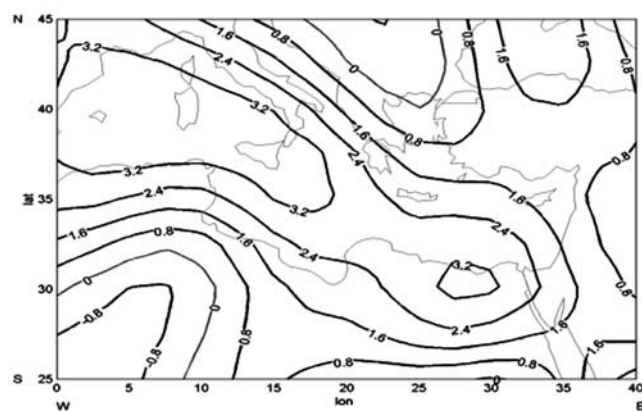


Figure 2. Long-term trend for the seasonal (JJA) 850 hPa temperature ($\text{K}/100\text{y}$) for 1948–2003, based on the slope of the best-fit straight line for each grid point.

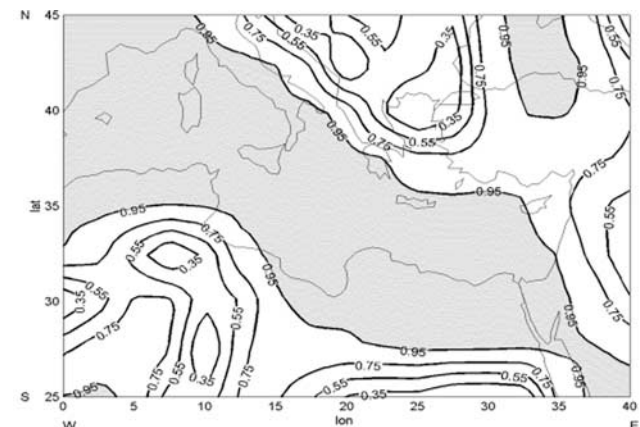


Figure 3. The spatial distribution of the confidence-level of the linear trend. Areas with confidence level >0.95 are shaded.

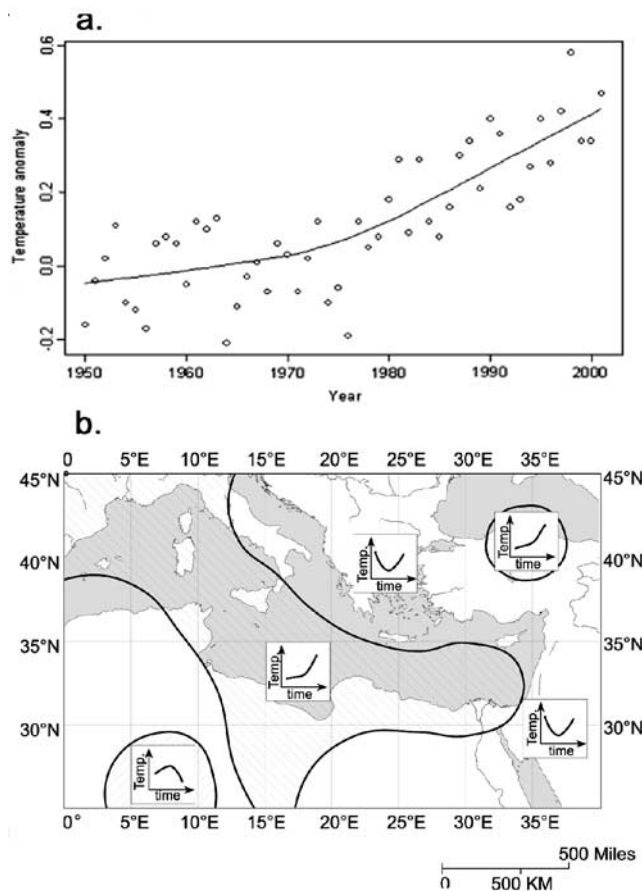


Figure 4. (a) Global surface yearly temperature (K) anomaly with respect to 1950–1980 average [IPCC, 2001] and the curve that approximates the long-term trend, using LOWESS method [Chambers *et al.*, 1983; Cleveland, 1979], with f-parameter of 0.8. (b) Spatial distribution of the shape of the long-term curve trends of the 850 hPa temperatures over the study region.

157 trend, where observed and that the reverse holds for the
158 cooling regions.

159 [12] The respective distribution for the 10% lower quan-
160 tile (not shown) indicates also a warming trend, implying a
161 reduction in cool days, over the warming region. However,
162 the warming trend of the lower tenth is rather smaller than
163 that of the upper tenth, suggesting that the temperature
164 regime is becoming more extreme there. An opposite trend
165 was found in the cooling regions.

166 4. Summary and Discussion

167 [13] The long-term trend of the summer temperature
168 regime (JJA) for 1948–2003 over the MB was studied.
169 The most prominent feature found is the long-term warming
170 over most of the study region, with a maximum of
171 0.04 Ky^{-1} over Sicily, i.e., 4 times larger than the global
172 average rate (0.01 Ky^{-1}). At the same time, cooling trend
173 was found over Algeria and over the Balkans.

174 [14] The magnitude of the linear long-term trend of the
175 10% upper quantile of the days was found larger than the
176 seasonal average in both the warming and cooling regions.
177 This implies that heat waves lead the general trend, and that

the regions subjected to general warming are also subjected
178 to an increasing burden of heat waves. Similar results, both
179 for the seasonal averages and the upper tenth days, were
180 found for each of the pertinent months separately, with July
181 being the most extreme. This tendency agrees with Meehl
182 and Tebaldi [2004] prediction for the 21st century.
183

[15] A similarity between the long-term course of the
184 global temperature and that over the majority of the MB,
185 was manifested by the long-term curve, combined of mild
186 warming up to the seventies, then gaining a pronounced
187 upward slope. This similarity was further validated by the
188 correlation between the global time-series and that averaged
189 over the region in the MB that has the same long-term
190 course, being +0.67. The respective correlation for the entire
191 Mediterranean Sea yielded also a significant correlation, of
192 +0.61.
193

[16] A comparison between the spatial distribution of
194 the long-term linear trend over the MB with the future
195 trend calculated by Meehl and Tebaldi [2004] indicates
196 that the regions which were found to cool, i.e., the Balkans
197 and Algeria, coincide more or less with the regions that
198 are expected to experience the most intense warming in
199 the 21st century. This trend reversal may be explained in
200 two alternative ways. One is that the observed cooling is
201 the negative phase of climatic oscillation, in which the
202 positive counterpart will take place on the 21st century and
203 other is that the climatic prediction model used missed a
204 regional unique process, which has caused cooling in these
205 regions.
206

[17] Simmons *et al.* [2004] showed that the NCEP/NCAR
207 data yielded a warming trend smaller than those obtained by
208 the CRU and the ERA-40 data sets for the period 1979–
209 2001, but an intermediate trend for the period 1958–2001.
210 The absence of a consistent error and the high inter-annual
211 correlations among the temperatures in these data sets for
212 Europe (>0.98 for each pair) [Simmons *et al.*, 2004] indicate
213 that our results are valid.
214

[18] In order to examine to what extent the 850 hPa
215 NCEP/NCAR gridded data fit the surface temperatures
216 based on GISS data used by Luterbacher *et al.* [2004] we
217 calculated the long-term linear trend for the region and
218 period they used ($35^{\circ}\text{N}–70^{\circ}\text{N}$, $25^{\circ}\text{W}–40^{\circ}\text{E}$, JJA 1976–
219 2003). We obtained $+0.050 \text{ Ky}^{-1}$ for the 850 hPa, which is
220

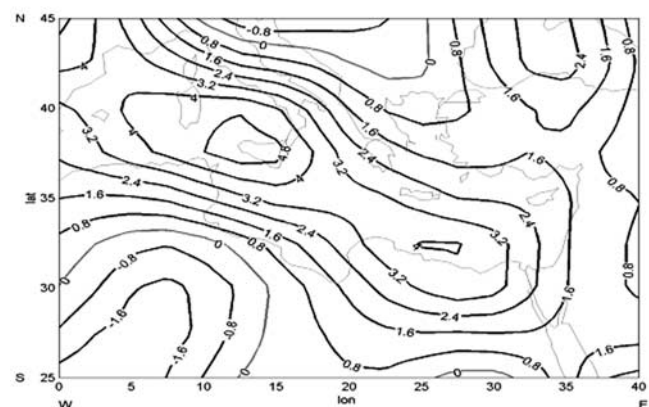


Figure 5. As for Figure 2 but for the upper tenth temperatures.

221 slightly smaller than the value of $+0.067 \text{ Ky}^{-1}$ they
 222 obtained for the surface air temperatures. This reflects a
 223 reasonable degree of agreement between both data sources
 224 and suggests that the difference may be attributed to the
 225 contribution of the urban effect.

226 [19] The magnitude of the warming trend over the MB,
 227 being considerably higher than the global one, suggests that
 228 synoptic scale factors may also play a significant role in that
 229 trend. Xoplaki et al. [2003] found that “three large-scale
 230 predictor fields (300 hPa geopotential height, 700–1000 hPa
 231 thickness and Mediterranean SSTs) account for more than
 232 50% of the total summer temperature variability”. We
 233 examined the long-term trend of the dynamic factors, which
 234 directly affect the temperature regime, i.e., vertical velocity
 235 and lower level advection. The only finding which partly
 236 supports the above hypothesis was a general weakening
 237 trend found in the 850 hPa wind speed for JJA (not shown),
 238 implying a weakening of the seasonal lower-level cool
 239 advection characterizing the MB [Alpert et al., 1990;
 240 Saaroni and Ziv, 2000; Saaroni et al., 2003; Ziv et al.,
 241 2004]. But, when this was examined for each of the
 242 pertinent months separately, no consistent trend was found.
 243 Furthermore, in July, in which the warming trend is the most
 244 pronounced, a strengthening of the lower level wind was
 245 observed. Regarding vertical velocity, over most of the
 246 warming regions a weakening trend of subsidence was
 247 found. We, therefore, cannot point at any dynamic factor
 248 that can explain the extreme warming trend found.

249 [20] The warming trend found in the summer season over
 250 the majority of the MB, the similarity between its long-term
 251 course and that of the global one and the absence of
 252 dynamic factors responsible for, suggest that the increase
 253 in the greenhouse effect, that affects the entire globe, affects
 254 also the MB in the summer, and even more intensely. This
 255 idea is supported by the clear sky in the summer season over
 256 the MB, which frees the region from a negative feedback of
 257 clouds. However, such an issue requires further, quantita-
 258 tive, investigation.

259 [21] The results and trends shown here indicate that the
 260 MB, which is subjected to a considerable heat stress in
 261 the summer season, may suffer from further aggravation in
 262 the summer heat stress and extreme heat waves that claim
 263 more lives, as happened in Western Europe in the summer
 264 of 2003. The warming process in dense populated regions is
 265 expected to be even faster near the surface due to the urban
 266 heat island, which is enhanced, at least partly, by energy
 267 emitted from air conditioners.

268 [22] **Acknowledgments.** This study is supported by the Israeli
 269 Science Foundation (ISF, grant no. 828/02). Partial support is due to the

GLOWA-JR funded by the BMBF and Min. of Sci. (MOS), Israel. Also, by 270
 the EU project DETECT. Special thanks are due to Orna Zafirir-Reuven for 271
 drawing Figure 4b. 272

References 273

- Alpert, P., R. Abramski, and B. U. Neeman (1990), The prevailing summer 274
 synoptic system in Israel—Subtropical high, not Persian trough, *Isr.* 275
J. Earth Sci., 39, 93–102. 276
- Chambers, J. M., W. S. Cleveland, B. Kleiner, and P. A. Tukey (1983), 277
Graphical Methods for Data Analysis, Wadsworth, Stamford, Conn. 278
- Cleveland, W. S. (1979), Robust locally weighted regression and smoothing 279
 scatterplots, *J. Am. Stat. Assoc.*, 74, 829–836. 280
- Intergovernmental Panel on Climate Change (IPCC) (2001), *Climate* 281
Change 2001: The Scientific Basis: Contribution of Working Group I 282
to the Third Assessment Report of the Intergovernmental Panel on 283
Climate Change, edited by J. T. Houghton et al., 881 pp., Cambridge 284
 Univ. Press, New York. 285
- Kalnay, E., and M. Cai (2003), Impact of urbanization and land-use change 286
 on climate, *Nature*, 423, 528–531. 287
- Kalnay, E., et al. (1996), The NCEP/NCAR 40-year reanalysis project, *Bull.* 288
Am. Meteorol. Soc., 77, 437–471. 289
- Kistler, R., et al. (2001), The NCEP/NCAR 50-year reanalysis: Monthly 290
 means CD-ROM and documentation, *Bull. Am. Meteorol. Soc.*, 82, 247– 291
 267. 292
- Le Comte, D. (2004), A year of extremes, *Weatherwise*, 57, 22–29. 293
- Luterbacher, J., D. Dietrich, E. Xoplaki, M. Grosjean, and H. Wanner 294
 (2004), European seasonal and annual temperature variability, trends, 295
 and extremes since 1500, *Science*, 303, 1499–1503, doi:10.1126/ 296
 science.1093877. 297
- Meehl, G., and C. Tebaldi (2004), More intense, more frequent, and longer 298
 lasting heat waves in the 21st century, *Science*, 305, 994–997. 299
- Reddaway, J. M., and G. R. Bigg (1996), Climatic change over the 300
 Mediterranean and links to the more general atmospheric circulation, 301
Int. J. Climatol., 16, 651–661. 302
- Saaroni, H., and B. Ziv (2000), Summer rainfall in a Mediterranean 303
 climate—The case of Israel: Climatological-dynamical analysis, *Int.* 304
J. Climatol., 20, 191–209. 305
- Saaroni, H., B. Ziv, J. Edelson, and P. Alpert (2003), Long-term variations 306
 in summer temperatures over the eastern Mediterranean, *Geophys. Res.* 307
Lett., 30(18), 1946, doi:10.1029/2003GL017742. 308
- Simmons, A. J., P. D. Jones, V. da Costa Bechtold, A. C. M. Beljaars, P. W. 309
 Källberg, S. Saarinen, S. M. Uppala, P. Viterbo, and N. Wedi (2004), 310
 Comparison of trends and variability in CRU, ERA-40 and NCEP/NCAR 311
 analyses of monthly-mean surface air temperature, *ERA-40 Proj. Rep.* 312
Ser.18, Eur. Cent. for Medium Range Weather Forecasts, Reading, UK. 313
- Wallen, C. C. (Ed.) (1977), *Climates of central and southern Europe*, in 314
World Survey of Climatology, vol. 6, Elsevier, New York. 315
- Xoplaki, E., J. F. Gonzalez-Rouco, J. Luterbacher, and H. Wanner (2003), 316
 Mediterranean summer air temperature variability and its connection to 317
 the large-scale atmospheric circulation and SSTs, *Clim. Dyn.*, 20, 723– 318
 739, doi:10.1007/s00382-003-0304-x. 319
- Ziv, B., H. Saaroni, and P. Alpert (2004), The factors governing the summer 320
 regime of the eastern Mediterranean, *Int. J. Climatol.*, 24, 1859–1871. 321

P. Alpert and A. Baharad, Department of Geophysics and Planetary 323
 Sciences, Tel-Aviv University, Tel-Aviv 69978, Israel. 324

H. Saaroni, Department of Geography and the Human Environment, 325
 Tel-Aviv University, Tel-Aviv 69978, Israel. (saaroni@post.tau.ac.il) 326

D. Yekutieli, Department of Statistics and Operations Research, Tel-Aviv 327
 University, Tel-Aviv 69978, Israel. 328

B. Ziv, Department of Natural Sciences, Open University of Israel, 329
 Tel-Aviv 61392, Israel. 330